Chemical Engineering Faculty Publication Series

Chemical Engineering

2021

Complex Coacervation of Polymerized Ionic Liquids in Non-acqueous Solvents

Minjung Lee
University of Massachusetts Amherst

Sarah L. Perry
University of Massachusetts Amherst

Ryan C. Hayward
University of Colorado, Boulder

Follow this and additional works at: https://scholarworks.umass.edu/che_faculty_pubs

Recommended Citation

Letter

Complex Coacervation of Polymerized Ionic Liquids in Non-aqueous Solvents

Minjung Lee, Sarah L. Perry, and Ryan C. Hayward*

Cite This: https://doi.org/10.1021/acspolymersau.1c00017

Read Online

ACCESS | Metrics & More | Article Recommendations | Supporting Information

ABSTRACT: Oppositely charged polymerized ionic liquids (PILs) were used to form complex coacervates in two different organic solvents, 2,2,2-trifluoroethanol (TFE) and hexafluoro-2-propanol (HFIP), and the corresponding phase diagrams were constructed using UV–vis, NMR, and turbidity experiments. While previous studies on complex coacervates have focused almost exclusively on aqueous environments, the use of PILs in the current work enabled studies in solvents with substantially lower dielectric constants (27.0 for TFE, 16.7 for HFIP). The critical salt concentration required to induce complete miscibility was roughly 2-fold larger in HFIP compared with TFE, and two different PIL complexes, solidlike precipitates and liquidlike coacervates, were found in both systems. This study provides insight into the effects of low-dielectric-constant solvents on complex coacervation, which has not been widely studied because of the limited solubility of conventional polyelectrolytes in these media.

KEYWORDS: polymerized ionic liquids, complex coacervates, low-dielectric-constant solvents, phase diagrams
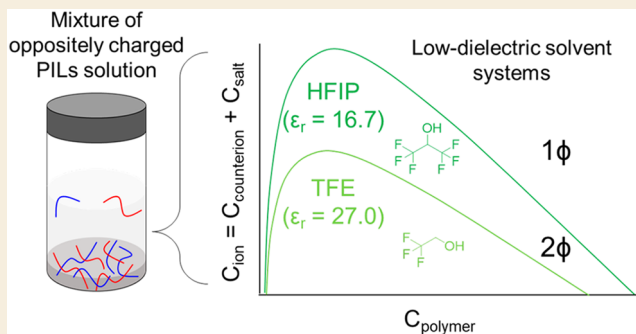
Complex coacervation is an active research topic because of its relevance in various fields such as food science,[1,2] biology,[3–6] biomedical science,[7,8] and polymer science[9–12] along with its importance in the behavior of a variety of natural[4,13,14] and synthetic[15–22] charged macromolecules. Over the past decade, major advances in our fundamental understanding of complex coacervation have been achieved using almost exclusively aqueous systems,[23,24] which provide good solubility for both weak[15–20,25–29] and strong polyelectrolyte pairs.[30–36] Specifically, systematic studies have focused on characterizing the influence of varying numerous parameters, including the polyanion/polycation ratio,[18,20,25] polymer chain length,[16,17,19,35,36] polymer chemistry,[22,29,35,37] salt choice,[26] pH,[18,25,28] and temperature.[18,38]

To date, however, there have been only a few studies on the effect of solvent quality on complex coacervation, and those that have been conducted are limited to aqueous mixtures with organic solvents.[15,21,34,39] Interestingly, increasing the volume ratio of organic solvent to water can either strengthen[15] or weaken[34] the salt resistance of coacervates depending on the choice of organic solvent and polyelectrolyte pair, although a detailed understanding of the underlying mechanisms to explain this variability is lacking. In one example, the addition of an organic solvent to an aqueous solution was found to convert the physical state of polyelectrolyte complexes formed from conjugated polyelectrolytes from solidlike precipitates to fluidlike coacervates as a result of the enhanced solubility of the polyelectrolyte pair in the organic solvent.[21] Very recently, the effect of solvent quality has been explored in aqueous

systems by comparing two polyelectrolyte pairs with different backbone chemistries: the hydrophobic polymers showed higher salt resistance than the hydrophilic polymer pair in water.[40] This experimental finding was in agreement with theoretical predictions of the coacervate phase diagrams that varied the effective Flory–Huggins parameter (χ) from poor to theta to good solvent. In addition to variations in the polymer backbone, changes in side-chain structure were found to impact coacervate phase behavior, including an increase in salt resistance driven by a decrease in local polarity.[22] Despite these findings, the effect of the solvent environment on complex coacervation has not been explored in the relatively low dielectric solvent regime ($\varepsilon_r \lesssim 30$) because of the scarcity of polyelectrolytes that are soluble in solvents with relatively low polarity. In high-dielectric environments, the entropic gain due to counterion release is understood to dominate coacervate formation.[15,41–44] Enthalpic effects due to interactions among the solvent, polymers, and counterions (captured in χ) can modulate this phase behavior,[34,35,40,45] but it remains unclear under which conditions the strength of electrostatic
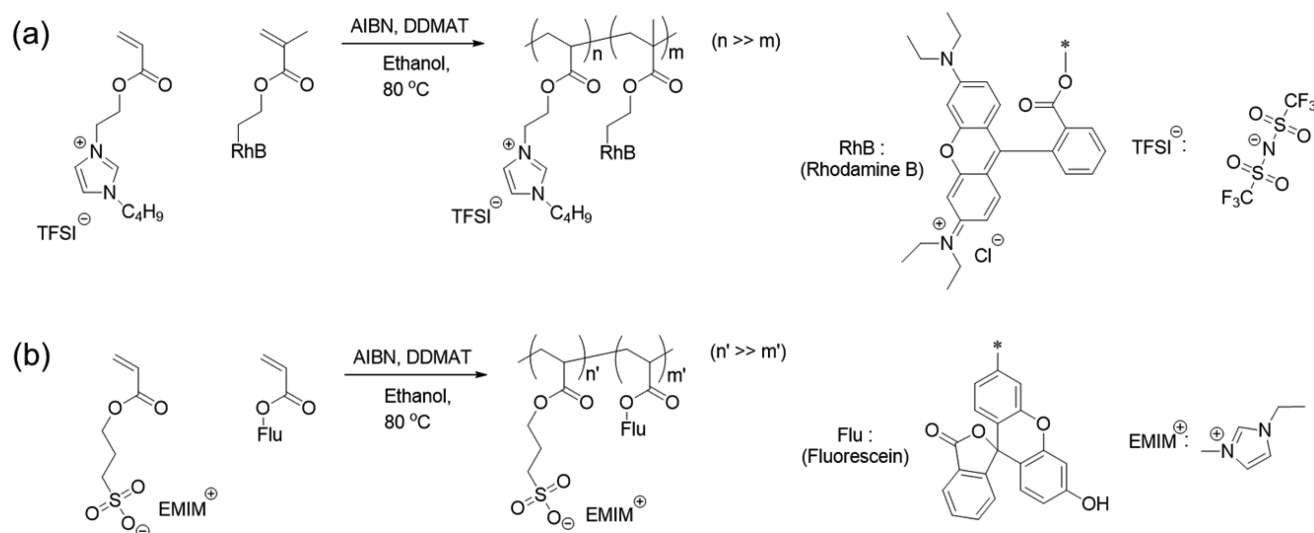
Figure 1. Synthesis of polymerized ionic liquids (PILs): (a) poly(AT-*co*-RhB) and (b) poly(ES-*co*-Flu).

interactions, e.g., as set by the solvent dielectric constant, will have a major influence.[42,46]

As a class of polyelectrolytes, polymerized ionic liquids (PILs) comprising ionic liquid moieties as both fixed ions and associated counterions enable studies in diverse solvent systems because of the relatively weak coordination between ions and the broad chemical tunability of both the polymer chain and counterion.[47−50] In particular, PILs can frequently be rendered soluble in nonaqueous solvents by introducing relatively nonpolar components such as hexafluorophosphate (PF_6^-) or bis(trifluoromethanesulfonyl)imide ($TFSI^-$) as either the polymerized ion or the counterion.[51] Although PIL systems have been mainly studied for various applications as ion conductors in electrochemical devices,[52−55] dispersants/surfactants,[56,57] carbon dioxide sorbents,[58,59] and anion-sensitive smart materials,[60,61] only a few studies of their behavior in the context of complex coacervation have been reported to date.[62,63]

In this work, we studied the complex coacervation of PILs in two organic solvents with low dielectric constants. For the resultant coacervate phase diagrams, we found a significant difference in the salt resistance of the two solvent systems and observed the formation of fluid coacervates and solid precipitates in both solvents. Here we discuss these findings in the context of enthalpy changes upon complexation, as dictated by Flory−Huggins interaction parameters (χ), as well as the possible influence of the solvent dielectric constant (ε_r).

To enable our study, we selected a pair of oppositely charged PILs, a polycation containing 1-(2-acryloyloxyethyl)-3-butylimidazolium bis(trifluoromethanesulfonyl)imide (AT) and a polyanion containing 1-ethyl-3-methylimidazolium 3-sulfopropyl acrylate (ES) (Figure 1). A small fraction (≤2 mol %) of a dye monomer (rhodamine B methacrylate or fluorescein *o*-acrylate) was incorporated into each PIL by RAFT polymerization, and both PILs were characterized by NMR spectroscopy (Figures S1 and S2). The molecular weights were estimated as M_n = 27 kDa for poly(AT-*co*-RhB) by size-exclusion chromatography with poly(methyl methacrylate) standards and M_n = 35−38 kDa for poly(ES-*co*-Flu) by ^{1}H NMR end-group analysis (see details in the Supporting Information (SI) and Figures S3 and S4). Given the much higher molecular weight of the AT monomer compared with

that of the standards, we note that this value is likely a significant underestimate. After screening several possible organic solvents, we identified two fluorinated alcohols, 2,2,2-trifluoroethanol (TFE) and hexafluoro-2-propanol (HFIP), that readily dissolved both PILs (up to approximately 10 wt %) and the salt. We note that the two solvents have relatively low dielectric constants at 300 K (ε_r = 27.0 for TFE[64,65] and 16.7 for HFIP[66,67]) compared with water[64] (ε_r = 78.0). For each solvent, separate solutions of the polycation and polyanion were first prepared with a chosen (and equal) concentration of polyelectrolyte $c_{poly(ES)} = c_{poly(AT)}$, expressed in terms of the molar concentration of ionizable monomeric units, as well as an additional amount c_{salt} of the ionic liquid 1-ethyl-3-methylimidazolium bis(trifluoromethanesulfonyl)imide ([EMIM][TFSI]), which corresponds to the salt formed by the two counterions. The two solutions were then rapidly mixed and allowed to equilibrate for at least 24 h prior to further characterization.

Because of the presence of fluorophores with well-resolved absorption spectra in the two PILs, it was possible to measure the concentration of each polymer in each phase using UV−vis spectroscopy (Figure 2). We first constructed a calibration curve for each PIL (Figure S5 and Table S1). The calibration curves of poly(AT-*co*-RhB) followed the Beer−Lambert equation ($A = \varepsilon lc + b$ with $b = 0$), whereas the calibration curves of poly(ES-*co*-Flu) required a nonzero intercept ($b \neq 0$). The reasons for this deviation from Beer−Lambert are not well-understood at present, but we note that in a prior report[68] the presence of an imidazolium-based IL was found to strongly suppress absorbance by fluorescein. Subsequently, the molar concentration of each PIL was obtained by measuring the UV−vis absorbance of each phase (Figure S6), dissolved in 2 M [EMIM][TFSI] solution for dilution/homogenization. The total polymer concentration $c_{polymer}$ in the phase diagrams was obtained by summation of the polycation and polyanion concentrations in each phase, $c_{polymer} = c_{poly(ES)} + c_{poly(AT)}$ (Table S2).

To determine the molar concentration of the TFSI anion in each phase, we used ^{19}F NMR spectroscopy, where the TFSI anion peak was distinguishable from other fluorine components in the mixtures (Figures S7−S9). The molar concentration of the EMIM cation in the two phases was
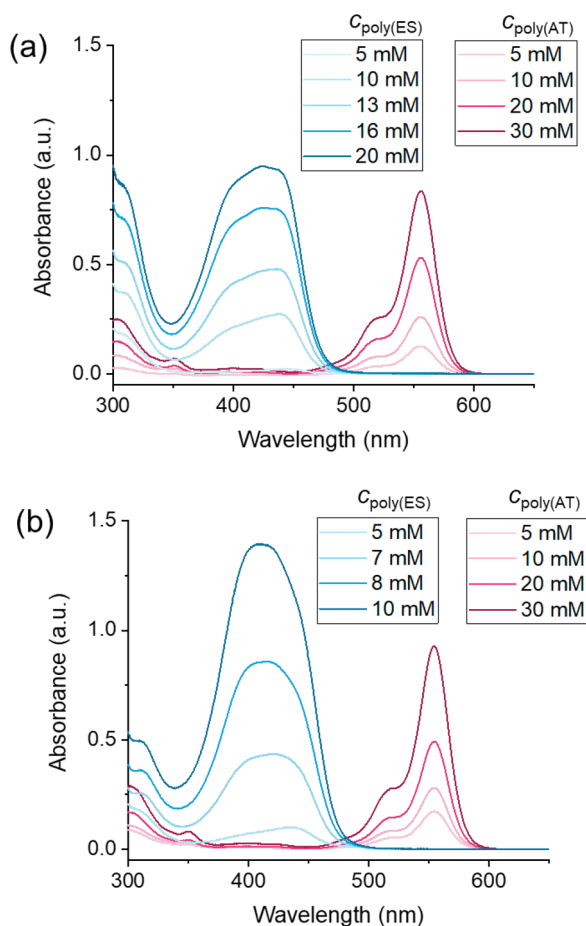
Figure 2. UV−vis absorption spectra of poly(AT-*co*-RhB) and poly(ES-*co*-Flu) solutions of varying polymer concentration in the range of 5−30 mM in (a) TFE and (b) HFIP with 2 M [EMIM][TFSI]. These calibration data were subsequently used to determine the polymer concentrations in each phase.

Figure 3. Turbidity measurements of PIL mixtures with different polymer concentrations (c_p) as a function of the added salt concentration (c_{salt}) in (a) TFE and (b) HFIP.

calculated by combining the UV−vis and ^{19}F NMR results in the equation $c_{EMIM} = c_{poly(ES)} + c_{TFSI} − c_{poly(AT)}$, which arises by assuming electroneutrality of each phase. The total concentration of small ions c_{ions} in the phase diagrams was obtained by summation of the TFSI and EMIM ion concentrations in each phase, $c_{ions} = c_{EMIM} + c_{TFSI}$ (Table S3), and includes both counterions and added salt. We also determined the compositions of the polymers and the small ions in each phase (Figures S10 and S11). Most notably, poly(ES) was found to preferentially partition into the dilute phase in both solvents, exceeding the concentration of poly(AT) by 10−20 mM. Although the origin of this effect is unclear, we speculate that it may arise from asymmetry in the molecular weights of the polymers or preferential interactions of the solvents with poly(ES) relative to poly(AT).

To determine the salt resistance, the turbidity (T) was measured by making three different samples with polymer concentrations in the range of 10−50 mM. The salt resistance was defined as the first point at which T dropped below 0.01, following a literature precedent.[16] As shown in Figure 3, the choice of solvent had a significant impact, with HFIP yielding a roughly 2-fold higher salt resistance than TFE ($c_{salt} \approx 600$ and 300 mM, respectively). The possible factors underlying this difference will be discussed further below.
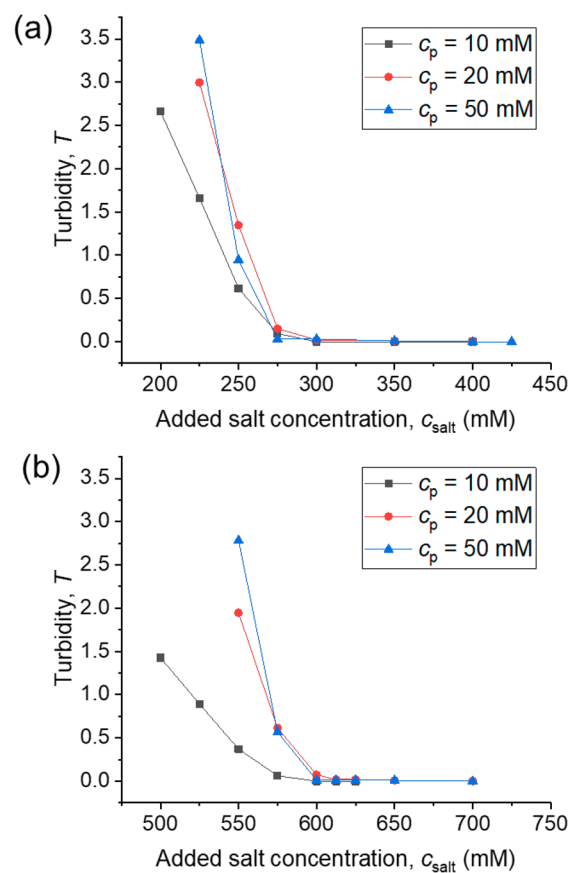
The coacervate phase diagrams of PILs in TFE and HFIP were constructed by combining the results of the UV−vis, ^{19}F NMR, and turbidity measurements (Figure 4). Several interesting observations from the phase diagrams can be made. First, there is a pronounced difference in the sizes of the two-phase regions for the two solvent systems. Specifically, the HFIP system has a higher salt resistance compared with the TFE system. One possible explanation is that the solvents may have different effective Flory−Huggins interaction parameters (χ) with the charged species, i.e., TFE is a better solvent than HFIP for the two polymers and associated counterions. However, swelling tests on cross-linked networks of each of the individual polyelectrolytes showed little difference between the two solvents (each containing 2 M [EMIM][TFSI]), suggesting that there is not a pronounced difference in the quality of the two solvents (see details in the SI and Figure S12).

Alternatively, the strength of electrostatic interactions, for example as captured in the Bjerrum length ($\lambda_B = e^2/(4\pi\varepsilon_r\varepsilon_0 k_B T)$), where $\lambda_B = 2.1$ nm in TFE and 3.4 nm in HFIP at 300 K (compared with 0.7 nm in water), may play a role in stabilizing coacervates to higher salt concentrations in HFIP than in TFE. Although theory has suggested that this electrostatic effect is negligible in high-polarity solvents ($\varepsilon_r \geq 60.0$),[46] the lower-polarity solvents employed here could potentially represent a different physical regime. For example, the degree of dissociation of ILs has been found to be relatively low in organic solvents with low dielectric constants.[69,70] This leads to tighter binding of counterions to the polymer chains as
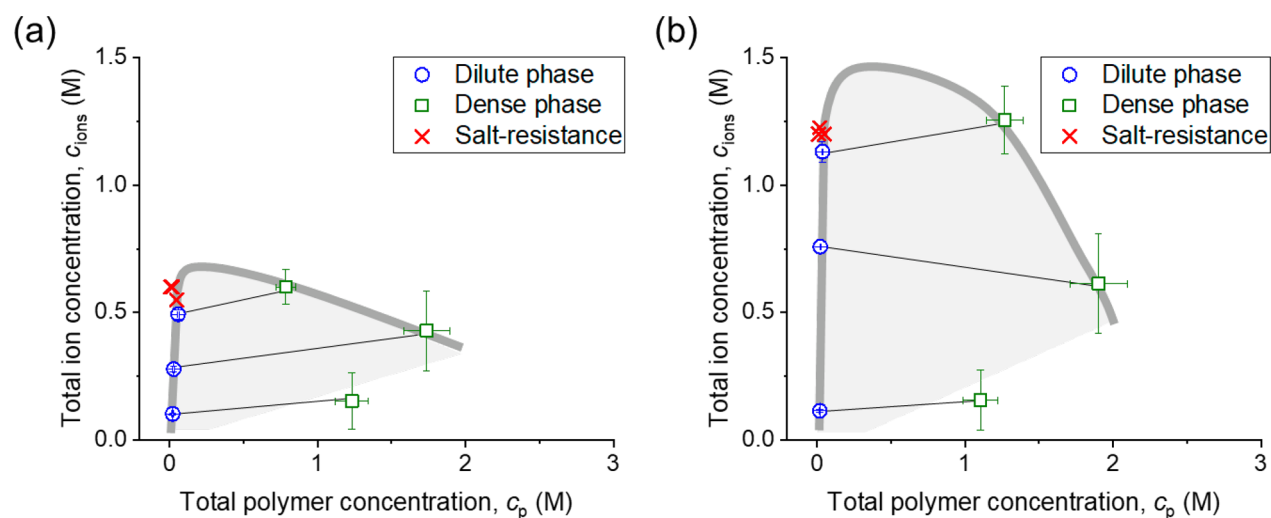
Figure 4. Complexation phase diagrams of PIL mixtures in (a) TFE and (b) HFIP, including the compositions of polymer-dilute (blue circles) and polymer-dense (green squares) phases and the salt-resistances (red crosses). The tie lines (black solid lines) connect the coexisting polymer-dilute and polymer-dense phases. Bold gray lines are estimated boundaries between single-phase (outside the boundaries) and two-phase regions (inside the boundaries, solid light gray).

well as a lower degree of dissociation of small ions in solution, presumably reducing both the entropic driving force for complex coacervates to form and the effect of added IL. Whether these effects have a net influence on coacervate stability in low-dielectric environments requires further study. The slopes of the tie lines relating the salt concentrations in the polymer-dense and polymer-dilute phases can in principle provide additional information. For example, positively sloped lines have been shown to correspond to a positive enthalpy change of complexation in aqueous systems.[45] Unfortunately, however, the uncertainties in the measured values of c_{ions} prevent us from reaching any conclusions with respect to the slopes of the tie lines in the phase diagrams presented here.

Finally, both solvent systems showed transitions in the physical states of the polymer-dense phases from solidlike precipitates to fluidlike coacervates and eventually to a homogeneous solution with increasing concentration of small ions, as reported previously for aqueous systems.[14,17,32,71] As expected, the solidlike precipitates were formed with no added salt or at low added salt concentrations, indicating that the PIL pairs have strong enough interactions in both solvents to form precipitates. These precipitates are kinetically trapped, as evidenced by their irregular (nonspherical) aggregates in contrast to the dispersed spherical droplets formed initially by coacervates (Figure S13).[7,30,72] In addition, even following 24 h of aging and subsequent centrifugation, polymer-dense phases with no added salt remained cloudy, while those at higher salt concentrations formed clear coacervate phases. Given the trapped nature of the solidlike precipitates at $c_{salt} = 0$, we do not extend the two-phase region in Figure 4 to low ion concentrations because of the lack of certainty about the equilibrium compositions of polymer-dense phases in this regime. A decrease in the concentration of the polymer in the polymer-dense phase with no (or low) added salt was found in both systems, which has been observed previously at the boundaries between solidlike precipitates and fluidlike coacervates and attributed to expansion of the polymer-dense phase by the solvent.[17,32,72,73]

In summary, two oppositely charged PILs were used to form complex coacervates in nonaqueous solvents with relatively

low dielectric constants ($\varepsilon_r = 27.0$ for TFE and 16.7 for HFIP). By combining UV–vis, ^{19}F NMR, and turbidity measurements, we constructed coacervate phase diagrams and confirmed that the solvent quality is an important parameter that can significantly alter the stability of coacervates upon addition of salts (i.e., [EMIM][TFSI] in this study), in agreement with previous studies.[15,34] In addition, both solvent systems showed two physical states of the polymer-dense phase (i.e., solidlike precipitates and fluidlike coacervates). Although we speculate that the origin of the different levels of salt stability is due to the influence of the low dielectric constant, further study is required to better understand this effect. In future studies, it will be interesting to expand the scope of experimental and theoretical studies of complex coacervation in waterless, hydrophobic environments to include a variety of different IL moieties and solvents, in addition to changing factors related to the polymers, e.g., the charge density. Such work may provide novel routes for processing of coacervate-based materials in non-aqueous solvents as well as new fundamental insight into complex coacervation by allowing for control over the level of dielectric mismatch between polymer-dense and polymer-dilute phases.[74−78]

■ ASSOCIATED CONTENT

Ⓢ Supporting Information

The Supporting Information is available free of charge at https://pubs.acs.org/doi/10.1021/acspolymersau.1c00017.

> Materials and methods, supporting text, Tables S1−S3, and Figures S1−S13 (PDF)

■ AUTHOR INFORMATION

Corresponding Author

Ryan C. Hayward − *Department of Polymer Science and Engineering, University of Massachusetts, Amherst, Amherst, Massachusetts 01003-9263, United States; Department of Chemical and Biological Engineering, University of Colorado Boulder, Boulder, Colorado 80309, United States;* ⓞ orcid.org/0000-0001-6483-2234; Email: Ryan.Hayward@colorado.edu

Authors

Minjung Lee − *Department of Polymer Science and Engineering, University of Massachusetts, Amherst, Amherst, Massachusetts 01003-9263, United States*

Sarah L. Perry − *Department of Chemical Engineering, University of Massachusetts, Amherst, Amherst, Massachusetts 01003-9303, United States;* ⓘ orcid.org/0000-0003-2301-6710

Complete contact information is available at:
https://pubs.acs.org/10.1021/acspolymersau.1c00017

■ REFERENCES

(1) Huang, G.-Q.; Du, Y.-L.; Xiao, J.-X.; Wang, G.-Y. Effect of Coacervation Conditions on the Viscoelastic Properties of N,O-Carboxymethyl Chitosan − Gum Arabic Coacervates. *Food Chem.* **2017**, *228*, 236−242.

(2) Santiago, L. G.; Castro, G. R. Novel Technologies for the Encapsulation of Bioactive Food Compounds. *Curr. Opin. Food Sci.* **2016**, *7*, 78−85.

(3) Aumiller, W. M.; Keating, C. D. Experimental Models for Dynamic Compartmentalization of Biomolecules in Liquid Organelles: Reversible Formation and Partitioning in Aqueous Biphasic Systems. *Adv. Colloid Interface Sci.* **2017**, *239*, 75−87.

(4) Aumiller, W. M.; Keating, C. D. Phosphorylation-Mediated RNA/Peptide Complex Coacervation as a Model for Intracellular Liquid Organelles. *Nat. Chem.* **2016**, *8* (2), 129−137.

(5) Kim, H. J.; Yang, B.; Park, T. Y.; Lim, S.; Cha, H. J. Complex Coacervates Based on Recombinant Mussel Adhesive Proteins: Their Characterization and Applications. *Soft Matter* **2017**, *13* (42), 7704−7716.

(6) Love, C.; Steinkühler, J.; Gonzales, D. T.; Yandrapalli, N.; Robinson, T.; Dimova, R.; Tang, T. -Y. D. Reversible PH-Responsive Coacervate Formation in Lipid Vesicles Activates Dormant Enzymatic Reactions. *Angew. Chem., Int. Ed.* **2020**, *59* (15), 5950−5957.

(7) Blocher, W. C.; Perry, S. L. Complex Coacervate-Based Materials for Biomedicine. *WIREs Nanomed Nanobiotechnol* **2017**, *9* (4), e1442.

(8) Ishii, S.; Kaneko, J.; Nagasaki, Y. Dual Stimuli-Responsive Redox-Active Injectable Gel by Polyion Complex Based Flower Micelles for Biomedical Applications. *Macromolecules* **2015**, *48* (9), 3088−3094.

(9) Zhou, D.; Pierucci, L.; Gao, Y.; O'Keeffe Ahern, J.; Huang, X.; Sigen, A.; Wang, W. Thermo- and PH-Responsive, Coacervate-Forming Hyperbranched Poly(β-Amino Ester)s for Selective Cell Binding. *ACS Appl. Mater. Interfaces* **2017**, *9* (7), 5793−5802.

(10) Lemmers, M.; Voets, I. K.; Cohen Stuart, M. A.; van der Gucht, J. Transient Network Topology of Interconnected Polyelectrolyte Complex Micelles. *Soft Matter* **2011**, *7* (4), 1378−1389.

(11) Hunt, J. N.; Feldman, K. E.; Lynd, N. A.; Deek, J.; Campos, L. M.; Spruell, J. M.; Hernandez, B. M.; Kramer, E. J.; Hawker, C. J. Tunable, High Modulus Hydrogels Driven by Ionic Coacervation. *Adv. Mater.* **2011**, *23* (20), 2327−2331.

(12) Lemmers, M.; Sprakel, J.; Voets, I. K.; van der Gucht, J.; Cohen Stuart, M. A. Multiresponsive Reversible Gels Based on Charge-Driven Assembly. *Angew. Chem., Int. Ed.* **2010**, *49* (4), 708−711.

(13) de Kruif, C. G.; Weinbreck, F.; de Vries, R. Complex Coacervation of Proteins and Anionic Polysaccharides. *Curr. Opin. Colloid Interface Sci.* **2004**, *9*, 340−349.

(14) Vieregg, J. R.; Lueckheide, M.; Marciel, A. B.; Leon, L.; Bologna, A. J.; Rivera, J. R.; Tirrell, M. V. Oligonucleotide−Peptide Complexes: Phase Control by Hybridization. *J. Am. Chem. Soc.* **2018**, *140* (5), 1632−1638.

(15) Chang, L.-W.; Lytle, T. K.; Radhakrishna, M.; Madinya, J. J.; Vélez, J.; Sing, C. E.; Perry, S. L. Sequence and Entropy-Based Control of Complex Coacervates. *Nat. Commun.* **2017**, *8* (1), No. 1273.

(16) Li, L.; Srivastava, S.; Andreev, M.; Marciel, A. B.; de Pablo, J. J.; Tirrell, M. V. Phase Behavior and Salt Partitioning in Polyelectrolyte Complex Coacervates. *Macromolecules* **2018**, *51* (8), 2988−2995.

(17) Chollakup, R.; Beck, J. B.; Dirnberger, K.; Tirrell, M.; Eisenbach, C. D. Polyelectrolyte Molecular Weight and Salt Effects on the Phase Behavior and Coacervation of Aqueous Solutions of Poly(Acrylic Acid) Sodium Salt and Poly(Allylamine) Hydrochloride. *Macromolecules* **2013**, *46* (6), 2376−2390.

(18) Chollakup, R.; Smitthipong, W.; Eisenbach, C. D.; Tirrell, M. Phase Behavior and Coacervation of Aqueous Poly(Acrylic Acid)−Poly(Allylamine) Solutions. *Macromolecules* **2010**, *43* (5), 2518−2528.

(19) Spruijt, E.; Westphal, A. H.; Borst, J. W.; Cohen Stuart, M. A.; van der Gucht, J. Binodal Compositions of Polyelectrolyte Complexes. *Macromolecules* **2010**, *43* (15), 6476−6484.

(20) Priftis, D.; Tirrell, M. Phase Behaviour and Complex Coacervation of Aqueous Polypeptide Solutions. *Soft Matter* **2012**, *8* (36), 9396−9405.

(21) Danielsen, S. P. O.; Nguyen, T.-Q.; Fredrickson, G. H.; Segalman, R. A. Complexation of a Conjugated Polyelectrolyte and Impact on Optoelectronic Properties. *ACS Macro Lett.* **2019**, *8* (1), 88−94.

(22) Lou, J.; Friedowitz, S.; Qin, J.; Xia, Y. Tunable Coacervation of Well-Defined Homologous Polyanions and Polycations by Local Polarity. *ACS Cent. Sci.* **2019**, *5* (3), 549−557.

(23) Srivastava, S.; Tirrell, M. V. Polyelectrolyte Complexation. *Adv. Chem. Phys.* **2016**, *161*, 499−544.

(24) Sing, C. E.; Perry, S. L. Recent Progress in the Science of Complex Coacervation. *Soft Matter* **2020**, *16* (12), 2885−2914.

(25) Priftis, D.; Xia, X.; Margossian, K. O.; Perry, S. L.; Leon, L.; Qin, J.; de Pablo, J. J.; Tirrell, M. Ternary, Tunable Polyelectrolyte Complex Fluids Driven by Complex Coacervation. *Macromolecules* **2014**, *47* (9), 3076−3085.

(26) Perry, S.; Li, Y.; Priftis, D.; Leon, L.; Tirrell, M. The Effect of Salt on the Complex Coacervation of Vinyl Polyelectrolytes. *Polymers* **2014**, *6* (6), 1756−1772.

(27) Marciel, A. B.; Srivastava, S.; Tirrell, M. V. Structure and Rheology of Polyelectrolyte Complex Coacervates. *Soft Matter* **2018**, *14* (13), 2454−2464.

(28) Li, L.; Srivastava, S.; Meng, S.; Ting, J. M.; Tirrell, M. V. Effects of Non-Electrostatic Intermolecular Interactions on the Phase Behavior of PH-Sensitive Polyelectrolyte Complexes. *Macromolecules* **2020**, *53* (18), 7835−7844.

(29) Tabandeh, S.; Leon, L. Engineering Peptide-Based Polyelectrolyte Complexes with Increased Hydrophobicity. *Molecules* **2019**, *24* (5), 868.

(30) Wu, H.; Ting, J. M.; Werba, O.; Meng, S.; Tirrell, M. V. Non-Equilibrium Phenomena and Kinetic Pathways in Self-Assembled Polyelectrolyte Complexes. *J. Chem. Phys.* **2018**, *149* (16), 163330.

(31) Schaaf, P.; Schlenoff, J. B. Saloplastics: Processing Compact Polyelectrolyte Complexes. *Adv. Mater.* **2015**, *27* (15), 2420−2432.

(32) Wang, Q.; Schlenoff, J. B. The Polyelectrolyte Complex/Coacervate Continuum. *Macromolecules* **2014**, *47* (9), 3108−3116.

(33) Fares, H. M.; Ghoussoub, Y. E.; Delgado, J. D.; Fu, J.; Urban, V. S.; Schlenoff, J. B. Scattering Neutrons along the Polyelectrolyte

Complex/Coacervate Continuum. *Macromolecules* **2018**, *51* (13), 4945−4955.

(34) Meng, S.; Liu, Y.; Yeo, J.; Ting, J. M.; Tirrell, M. V. Effect of Mixed Solvents on Polyelectrolyte Complexes with Salt. *Colloid Polym. Sci.* **2020**, *298* (7), 887−894.

(35) Liu, Y.; Santa Chalarca, C. F.; Carmean, R. N.; Olson, R. A.; Madinya, J.; Sumerlin, B. S.; Sing, C. E.; Emrick, T.; Perry, S. L. Effect of Polymer Chemistry on the Linear Viscoelasticity of Complex Coacervates. *Macromolecules* **2020**, *53* (18), 7851−7864.

(36) Meng, X.; Du, Y.; Liu, Y.; Coughlin, E. B.; Perry, S. L.; Schiffman, J. D. Electrospinning Fibers from Oligomeric Complex Coacervates: No Chain Entanglements Needed. *Macromolecules* **2021**, *54* (11), 5033−5042.

(37) Huang, J.; Morin, F. J.; Laaser, J. E. Charge-Density-Dominated Phase Behavior and Viscoelasticity of Polyelectrolyte Complex Coacervates. *Macromolecules* **2019**, *52* (13), 4957−4967.

(38) Ali, S.; Bleuel, M.; Prabhu, V. M. Lower Critical Solution Temperature in Polyelectrolyte Complex Coacervates. *ACS Macro Lett.* **2019**, *8* (3), 289−293.

(39) Sun, J.; Perry, S. L.; Schiffman, J. D. Electrospinning Nanofibers from Chitosan/Hyaluronic Acid Complex Coacervates. *Biomacromolecules* **2019**, *20* (11), 4191−4198.

(40) Li, L.; Rumyantsev, A. M.; Srivastava, S.; Meng, S.; de Pablo, J. J.; Tirrell, M. V. Effect of Solvent Quality on the Phase Behavior of Polyelectrolyte Complexes. *Macromolecules* **2021**, *54*, 105−114.

(41) Priftis, D.; Laugel, N.; Tirrell, M. Thermodynamic Characterization of Polypeptide Complex Coacervation. *Langmuir* **2012**, *28* (45), 15947−15957.

(42) Fu, J.; Schlenoff, J. B. Driving Forces for Oppositely Charged Polyion Association in Aqueous Solutions: Enthalpic, Entropic, but Not Electrostatic. *J. Am. Chem. Soc.* **2016**, *138* (3), 980−990.

(43) Priftis, D.; Megley, K.; Laugel, N.; Tirrell, M. Complex Coacervation of Poly(Ethylene-Imine)/Polypeptide Aqueous Solutions: Thermodynamic and Rheological Characterization. *J. Colloid Interface Sci.* **2013**, *398*, 39−50.

(44) Kayitmazer, A. B. Thermodynamics of Complex Coacervation. *Adv. Colloid Interface Sci.* **2017**, *239*, 169−177.

(45) Schlenoff, J. B.; Yang, M.; Digby, Z. A.; Wang, Q. Ion Content of Polyelectrolyte Complex Coacervates and the Donnan Equilibrium. *Macromolecules* **2019**, *52* (23), 9149−9159.

(46) Lytle, T. K.; Sing, C. E. Transfer Matrix Theory of Polymer Complex Coacervation. *Soft Matter* **2017**, *13* (39), 7001−7012.

(47) Yuan, J.; Antonietti, M. Poly(Ionic Liquid)s: Polymers Expanding Classical Property Profiles. *Polymer* **2011**, *52* (7), 1469−1482.

(48) Mecerreyes, D. Polymeric Ionic Liquids: Broadening the Properties and Applications of Polyelectrolytes. *Prog. Polym. Sci.* **2011**, *36* (12), 1629−1648.

(49) Yuan, J.; Mecerreyes, D.; Antonietti, M. Poly(Ionic Liquid)s: An Update. *Prog. Polym. Sci.* **2013**, *38* (7), 1009−1036.

(50) Qian, W.; Texter, J.; Yan, F. Frontiers in Poly(Ionic Liquid)s: Syntheses and Applications. *Chem. Soc. Rev.* **2017**, *46* (4), 1124−1159.

(51) Marcilla, R.; Alberto Blazquez, J.; Rodriguez, J.; Pomposo, J. A.; Mecerreyes, D. Tuning the Solubility of Polymerized Ionic Liquids by Simple Anion-Exchange Reactions. *J. Polym. Sci., Part A: Polym. Chem.* **2004**, *42* (1), 208−212.

(52) Lin, B.; Feng, T.; Chu, F.; Zhang, S.; Yuan, N.; Qiao, G.; Ding, J. Poly(Ionic Liquid)/Ionic Liquid/Graphene Oxide Composite Quasi Solid-State Electrolytes for Dye Sensitized Solar Cells. *RSC Adv.* **2015**, *5* (70), 57216−57222.

(53) Tiruye, G. A.; Muñoz-Torrero, D.; Palma, J.; Anderson, M.; Marcilla, R. Performance of Solid State Supercapacitors Based on Polymer Electrolytes Containing Different Ionic Liquids. *J. Power Sources* **2016**, *326*, 560−568.

(54) Gu, L.; Dong, H.; Sun, Z.; Li, Y.; Yan, F. Spirocyclic Quaternary Ammonium Cations for Alkaline Anion Exchange Membrane Applications: An Experimental and Theoretical Study. *RSC Adv.* **2016**, *6* (97), 94387−94398.

(55) Lu, F.; Gao, X.; Wu, A.; Sun, N.; Shi, L.; Zheng, L. Lithium-Containing Zwitterionic Poly(Ionic Liquid)s as Polymer Electrolytes for Lithium-Ion Batteries. *J. Phys. Chem. C* **2017**, *121* (33), 17756−17763.

(56) Kim, T. Y.; Lee, T. H.; Kim, J. E.; Kasi, R. M.; Sung, C. S. P.; Suh, K. S. Organic Solvent Dispersion of Poly(3,4-Ethylenedioxythiophene) with the Use of Polymeric Ionic Liquid: Organic Solvent Dispersion of Pedot. *J. Polym. Sci., Part A: Polym. Chem.* **2008**, *46* (20), 6872−6879.

(57) Ager, D.; Arjunan Vasantha, V.; Crombez, R.; Texter, J. Aqueous Graphene Dispersions−Optical Properties and Stimuli-Responsive Phase Transfer. *ACS Nano* **2014**, *8* (11), 11191−11205.

(58) Voss, B. A.; Bara, J. E.; Gin, D. L.; Noble, R. D. Physically Gelled Ionic Liquids: Solid Membrane Materials with Liquidlike CO_2 Gas Transport. *Chem. Mater.* **2009**, *21* (14), 3027−3029.

(59) Soll, S.; Zhang, P.; Zhao, Q.; Wang, Y.; Yuan, J. Mesoporous Zwitterionic Poly(Ionic Liquid)s: Intrinsic Complexation and Efficient Catalytic Fixation of CO_2. *Polym. Chem.* **2013**, *4* (19), 5048.

(60) He, X.; Yang, W.; Pei, X. Preparation, Characterization, and Tunable Wettability of Poly(Ionic Liquid) Brushes via Surface-Initiated Atom Transfer Radical Polymerization. *Macromolecules* **2008**, *41* (13), 4615−4621.

(61) Texter, J. Anion Responsive Imidazolium-Based Polymers. *Macromol. Rapid Commun.* **2012**, *33* (23), 1996−2014.

(62) Shah, A.; Kuddushi, M.; Rajput, S.; El Seoud, O. A.; Malek, N. I. Ionic Liquid-Based Catanionic Coacervates: Novel Microreactors for Membrane-Free Sequestration of Dyes and Curcumin. *ACS Omega* **2018**, *3* (12), 17751−17761.

(63) Shah, A.; Kuddushi, M.; Ray, D.; Aswal, V. K.; Malek, N. I. Sodium Salicylate Mediated Ionic Liquid Based Catanionic Coacervates as Membrane-Free Microreactors for the Selective Sequestration of Dyes and Curcumin. *ChemSystemsChem* **2020**, *2* (3), No. e1900029.

(64) Chitra, R.; Smith, P. E. Properties of 2,2,2-Trifluoroethanol and Water Mixtures. *J. Chem. Phys.* **2001**, *114* (1), 426.

(65) Berkland, C. Controlling Surface Nano-Structure Using Flow-Limited Field-Injection Electrostatic Spraying (FFESS) of Poly(D,L-lactide-co-glycolide). *Biomaterials* **2004**, *25* (25), 5649−5658.

(66) Mayans, E.; Ballano, G.; Sendros, J.; Font-Bardia, M.; Campos, J. L.; Puiggalí, J.; Cativiela, C.; Alemán, C. Effect of Solvent Choice on the Self-Assembly Properties of a Diphenylalanine Amphiphile Stabilized by an Ion Pair. *ChemPhysChem* **2017**, *18* (14), 1888−1896.

(67) Carraro, M.; Gardan, M.; Sartorel, A.; Maccato, C.; Bonchio, M. Hydrogen Peroxide Activation by Fluorophilic Polyoxotungstates for Fast and Selective Oxygen Transfer Catalysis. *Dalton Transactions* **2016**, *45*, 14544−14548.

(68) Ali, M.; Dutta, P.; Pandey, S. Effect of Ionic Liquid on Prototropic and Solvatochromic Behavior of Fluorescein. *J. Phys. Chem. B* **2010**, *114* (46), 15042−15051.

(69) Li, W.; Zhang, Z.; Han, B.; Hu, S.; Xie, Y.; Yang, G. Effect of Water and Organic Solvents on the Ionic Dissociation of Ionic Liquids. *J. Phys. Chem. B* **2007**, *111* (23), 6452−6456.

(70) Tokuda, H.; Baek, S.-J.; Watanabe, M. Room-Temperature Ionic Liquid-Organic Solvent Mixtures: Conductivity and Ionic Association. *Electrochemistry* **2005**, *73*, 620−622.

(71) Liu, Y.; Momani, B.; Winter, H. H.; Perry, S. L. Rheological Characterization of Liquid-to-Solid Transitions in Bulk Polyelectrolyte Complexes. *Soft Matter* **2017**, *13* (40), 7332−7340.

(72) Meng, S.; Ting, J. M.; Wu, H.; Tirrell, M. V. Solid-to-Liquid Phase Transition in Polyelectrolyte Complexes. *Macromolecules* **2020**, *53* (18), 7944−7953.

(73) Shamoun, R. F.; Reisch, A.; Schlenoff, J. B. Extruded Saloplastic Polyelectrolyte Complexes. *Adv. Funct. Mater.* **2012**, *22* (9), 1923−1931.

(74) Wei, Y.; Chiang, P.; Sridhar, S. Ion Size Effects on the Dynamic and Static Dielectric Properties of Aqueous Alkali Solutions. *J. Chem. Phys.* **1992**, *96* (6), 4569−4573.

F

(75) Levy, A.; Andelman, D.; Orland, H. Dielectric Constant of Ionic Solutions: A Field-Theory Approach. *Phys. Rev. Lett.* **2012**, *108* (22), 227801.

(76) Kumar, R.; Sumpter, B. G.; Muthukumar, M. Enhanced Phase Segregation Induced by Dipolar Interactions in Polymer Blends. *Macromolecules* **2014**, *47* (18), 6491−6502.

(77) Jing, Y.; Jadhao, V.; Zwanikken, J. W.; Olvera de la Cruz, M. Ionic Structure in Liquids Confined by Dielectric Interfaces. *J. Chem. Phys.* **2015**, *143* (19), 194508.

(78) Nguyen, T. D.; Olvera de la Cruz, M. Manipulation of Confined Polyelectrolyte Conformations through Dielectric Mismatch. *ACS Nano* **2019**, *13* (8), 9298−9305.